Effect of uniaxial stress on the $H_A(Li^+)$ center in KCl:Li^+: Change of center geometry by ⟨100⟩ stress*

Dirk Schoemaker
Argonne National Laboratory, Argonne, Illinois 60439
Physics Department, University of Antwerp (U.I.A.), 2610-Wilrijk, Belgium†
(Received 13 September 1973)

With no applied external uniaxial stress the Cl_2^- axis of the $H_A(Li^+)$ center in KCl:Li^+ makes a 26° angle with [100] in the (110) plane. It is shown through an analysis of the electron-paramagnetic-resonance spectra that [001] uniaxial stress changes the geometry of the $H_A(Li^+)$ center at low temperatures. The Cl_2^- axis moves out of the (110) plane and with increasing stress describes an octant of a cone around [100] having a $2\times26° = 52°$ apex angle. At high uniaxial stresses ($\sim 5\times10^8$ dyn/cm^2) and at 4.2 K the Cl_2^- axis is within a few degrees of the (001) plane. Raising the temperature above 4.2 K counteracts the effect of the uniaxial stress while lowering the temperature aids it. Above ~50 K the [001] uniaxial stress is no longer effective in changing the $H_A(Li^+)$ center geometry. The stressed $H_A(Li^+)$ center possesses a restricted interstitial motion (RIM) which, similar to the RIM of the unstressed $H_A(Li^+)$ center, may be tunneling a low temperatures.

I. INTRODUCTION

In two previous papers,[1,2] hereafter called I and II, the structure and the motional properties of the $H_A(Li^+)$ center in KCl : Li^+ have been described in detail. In I it was shown from electron-paramagnetic-resonance (EPR) and optical-absorption measurements that $H_A(Li^+)$ is an interstitial halogen-atom center[3] which manifests itself as a Cl_2^- molecule ion occupying a single negative-ion site next to a substitutional Li^+ ion. The Cl_2^- internuclear axis makes a 26° angle with ⟨100⟩ in a {110} plane. In II it was shown that $H_A(Li^+)$ possesses two well-defined reorientation motions called the pyramidal motion (PM) and the restricted interstitial motion (RIM), respectively. In the PM the Cl_2^- molecular bond is maintained and the Cl_2^- jumps among the four possible equivalent orientations around a given ⟨100⟩. In the RIM the interstitial Cl atom exchanges molecular bonds with the three substitutional Cl^- ions that surround it. This motion takes place around ⟨111⟩ and possesses C_{3v} symmetry.

The RIM proved to be particularly interesting because, as demonstrated in II, it is tunneling at low temperatures. Consequently, it was decided to study this tunneling motion by means of uniaxial stress at liquid-helium temperatures. Two stress directions were studied, viz., $\vec{\sigma} \parallel \langle 100\rangle$ and[4] $\vec{\sigma} \parallel \langle 110\rangle$, with, in both cases, the stress $\vec{\sigma}$ perpendicular to the static magnetic field $\vec{H}$ used in the EPR experiments. The results were unexpected and surprising. Briefly, the following was observed: ⟨100⟩ uniaxial stress changes the *geometric* structure of the $H_A(Li^+)$ center drastically and this effect completely overpowers any effect that $\vec{\sigma}$ could have had on the degeneracy of the tunneling orientations. A ⟨110⟩ stress, on the other hand, does lift the degeneracy of the tunneling orientations[4] but does *not* affect the $H_A(Li^+)$ geometry. As a result of this qualitative difference the two stress configurations will be dealt with in different papers. This paper then will be limited to the discussion of the $\vec{\sigma} \parallel \langle 100\rangle$ experiments.

II. EXPERIMENTAL

Details on sample preparation, EPR measurements, etc., have been given before.[1,2] For the uniaxial-stress measurements, the small cylindrical fused-silica EPR cavity was somewhat modified. Just below the bottom of the center of the cavity a solid metal part, playing the role of an anvil, was suspended independently of the cavity body, so that small displacements or deformations resulting from a force applied to it would affect the tuning of the cavity as little as possible. The KCl : Li^+ sample was contained in a small Teflon tube (~ 7 cm long) with one open end. On the bottom of this tube was placed first a short (~ 2-mm) piece of cylindrical fused silica with polished faces, which fitted snugly into the tube. Then came the KCl : Li^+ sample (usually ~ 10 mm long) and on top of the sample again a short piece of fused silica with polished faces. The top of the Teflon tube slid over a long (~ 1-m) stainless-steel tube so that the sample could be inserted or taken out of the cavity through the top of the Andonian variable-temperature Dewar which contained the cavity. Stress was then applied through a somewhat longer metal rod passing through the stainless-steel tube and resting on the upper piece of fused silica in the Teflon holder. The long metal rod was connected to the plunger of an air piston which was driven by the high pressure from a nitrogen tank. The maximum uniaxial stress that could be generated with this setup was about 5.5×10^8 dyn/cm^2, which was

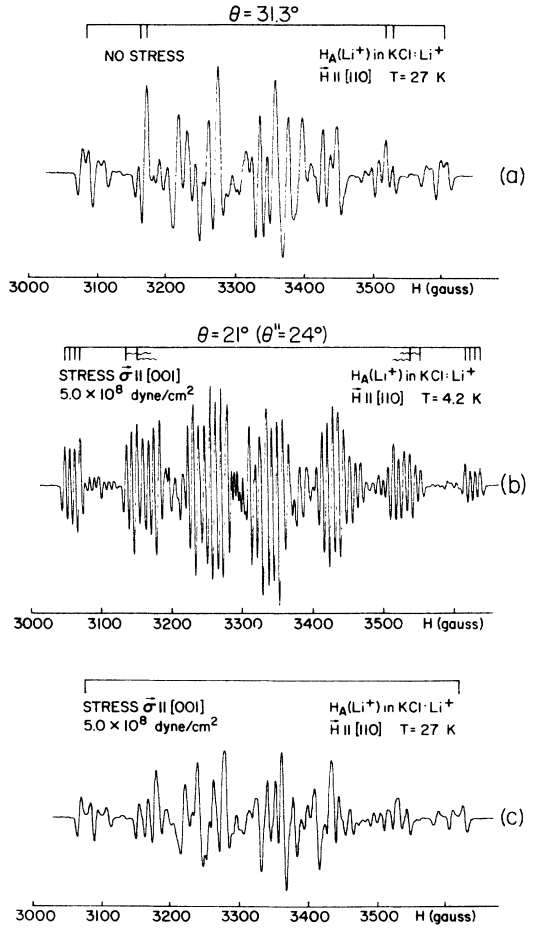

FIG. 1. (a) $H_A(Li^+)$-center EPR spectrum at 27 K for $\vec{H}$ ∥ [110] and without uniaxial stress; (b) same spectrum but with 5×10^8 dyn/cm^2 uniaxial stress along [001] and at 4.2 K; (c) same as (b) but at 27 K. The second derivative of the absorption is presented.

just about what the samples would tolerate at low temperatures.

III. EXPERIMENTAL RESULTS AND DISCUSSION

A. $H_A(Li^+)$ EPR spectrum under ⟨100⟩ uniaxial stress

Figure 1 presents the $\vec{H}$ ∥ [110] EPR spectra of $H_A(Li^+)$ with and without $\vec{\sigma}$ ∥ [001] uniaxial stress. The magnitude of the stress was about 5×10^8 dyn/cm^2. This was not only the maximum stress available with our stress apparatus but was also about the maximum stress that the crystal would tolerate. The $\vec{H}$ ∥ [110] spectrum without stress was taken at a temperature above 15 K and the reason for this will be given in another paper.[5] Figure 2 gives the two spectra for $\vec{H}$ ∥ [100], both at 4.2 K. For convenience we will call the $H_A(Li^+)$ under uniaxial stress a "stressed $H_A(Li^+)$ center" with a similar definition for "unstressed $H_A(Li^+)$ center."

The unstressed $\vec{H}$ ∥ [100] EPR spectrum in Fig. 2 shows clearly the seven-line hyperfine (hf) pattern which is characteristic of a Cl_2^- molecule ion. This seven-line hf pattern is also observed in the unstressed $\vec{H}$ ∥ [110] spectrum in Fig. 1(a), but in this case the EPR lines possess also unresolved superhyperfine (shf) structure. In I this shf was shown to originate from the nuclei of the two substitutional Cl^- ions, Nos. 3 and 4 in Fig. 3. In II it was shown that these substitutional ions play an important role in the RIM.

The $\vec{H}$ ∥ [110] EPR spectrum when $\vec{\sigma}$ ∥ [001] uniaxial stress is applied [Fig. 1(b)], is qualitatively very different from the unstressed EPR spectrum. Nevertheless a seven-line hf structure is still clearly evident, indicating that the $H_A(Li^+)$ center remains a Cl_2^- molecule ion under stress. A four-line shf structure has become clearly resolved [see the highest and the lowest field lines of Fig. 1(b)] and one concludes that $H_A(Li^+)$ under stress possesses a shf interaction with only one Cl nucleus. (Both Cl isotopes, ^{35}Cl and ^{37}Cl, possess nuclear spin $\frac{3}{2}$ and comparable nuclear moments.)

With this high value for the uniaxial stress ($\sigma = 5\times10^8$ dyn/cm^2), an angular-variation study of the spectrum was made in the (001) plane perpendicular to the $\vec{\sigma}$ ∥ [001] stress direction. It was found that the over-all seven-line hf structure reached a maximum when the magnetic field $\vec{H}$ made a $\theta' = 24° \pm 1°$ angle with [100] in the (001) plane. The magnitude of this maximum splitting was measured to be 605.4 G. This corresponds to an average hf splitting of $\frac{1}{6}\times605.4 = 100.9$ G,

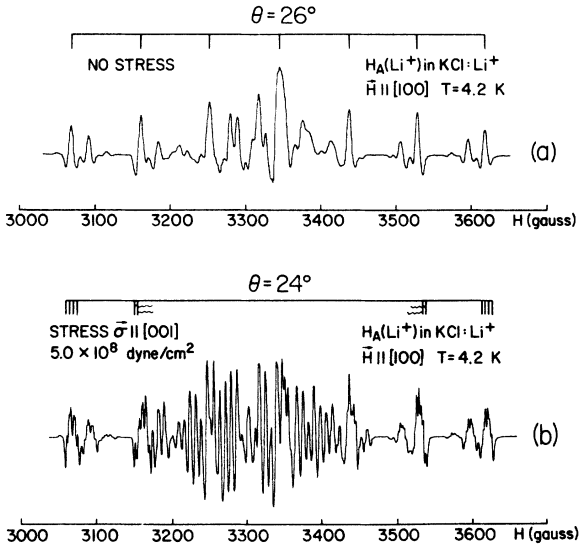

FIG. 2. (a) $H_A(Li^+)$-center EPR spectrum at 4.2 K for $\vec{H}$ ∥ [100] and without uniaxial stress; (b) same spectrum but with 5×10^8 dyn/cm^2 uniaxial stress along [001]. The second derivative of the absorption is presented.

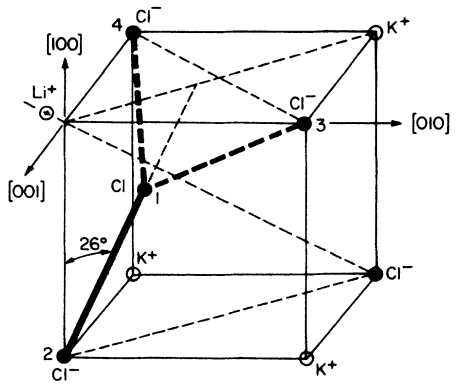

FIG. 3. Schematic three-dimensional representation of the unstressed $H_A(Li^+)$ center in KCl : Li^+.

and this is close to the value which is normally observed when the magnetic field is parallel to the Cl_2^- molecular axis; e.g., for the unstressed $H_A(Li^+)$ center the average hf splitting is 101.5 G when $\vec{H}$ is parallel to the Cl_2^- internuclear axis z''. One is led to conclude then that the $\vec{\sigma} \parallel [001]$ uniaxial stress has pushed the Cl_2^- internuclear axis out of the (011) plane into, or very close to, the (001) plane perpendicular to the stress direction, with the Cl_2^- axis making a $\theta' = 24°$ angle with the [100] direction. The quantitative analysis taking into account all the stressed EPR spectra $\{\vec{H} \parallel [100]$; $\vec{H} \parallel [110]$; $\vec{H} \parallel [100] + 24°$ in (001)$\}$ confirms this.

The stressed $H_A(Li^+)$ EPR spectra were matched to the following spin Hamiltonian:

$$\frac{\mathcal{H}}{g_0 \mu_B} = \frac{1}{g_0} \vec{H} \cdot \vec{g} \cdot \vec{S} + \sum_{i=1}^{4} \vec{S} \cdot \vec{A}_i \cdot \vec{I}_i ,$$

in which the $\vec{g}$ and $\vec{A}_i$ tensor axes were allowed to have different orientations in the (001) plane. In order to make the quantitative analysis feasible the following very reasonable assumptions were made: (a) axial symmetry for $\vec{g}$ and $\vec{A}_i$; (b) the symmetry axis of $\vec{g}$ coincides with the direction of the internuclear axis z'', which is taken as the direction of maximum hf interaction, i.e., 24° away from [100] in (001); (c) the Cl_2^- bond is bent symmetrically, i.e., the symmetry axes of $\vec{A}_1$ and $\vec{A}_2$ make angles δ and $-\delta$ with the internuclear axis; (d) the perpendicular components of $\vec{A}_1$ and $\vec{A}_2$ were chosen to be the same as for the unstressed $H_A(Li^+)$ center, namely, $A_{\perp 1} \cong 14$ G and $A_{\perp 2} \cong 8$ G. The results of the analysis with these assumptions are summarized in Table I. It was found in particular that the two Cl nuclei of the basic Cl_2^- are inequivalent and that the molecular bond is bent by $15° \pm 3°$. The shf interaction with the third Cl nucleus could also be analyzed approximately and it was determined that the symmetry axis of $\vec{A}_3$ makes a $17° \pm 5°$ angle with [010] in the (001) plane.

TABLE I. Spin-Hamiltonian parameters of the $^{35}Cl_2^-$ $H_A(Li^+)$ center in KCl : Li^+ under very high [001] uniaxial stress (5×10^8 dyn/cm^2) at 4.2 K [see Figs. 4(b) and 5(a)]. For comparison the parameters of the unstressed $H_A(Li^+)$ center (Fig. 3) are also given. The hyperfine parameters and the linewidth ΔH (between the extrema of the first derivative) are given in gauss. δ is the bending angle of the Cl_2^- molecule ion.

Center	$g_\parallel$	$g_\perp$	$A_{\parallel 1,2}$	$A_{\perp 1,2}$	$A_{\parallel 3,4}$	$A_{\perp 3,4}$	δ	ΔH
Stressed $H_A(Li^+)$[a]	2.0036[b] ± 0.0010	2.031 ± 0.004	$A_{\parallel,1}$[c] = 108.2 ± 0.5 $A_{\parallel,2}$[e] = 94.7 ± 0.5	($A_{\perp,1}$ = 14) ($A_{\perp,2}$ = 8)	$A_{\parallel,3}$[d] = 8.5 ± 0.5 $A_{\parallel,5} \leq 2$	...	15° ± 3°	3.9 ± 0.4
Unstressed $H_A(Li^+)$[f]	2.0020 ± 0.0004	2.031 ± 0.002	$A_{\parallel,1}$ = 106.5 ± 0.5 $A_{\parallel,2}$ = 96.5 ± 0.5	$A_{\perp,1}$ = 14 ± 5 $A_{\perp,2}$ = 8 ± 5	$A_{\parallel,3} \equiv A_{\parallel,4}$ = 4.2 ± 0.5	$A_{\perp,3} \equiv A_{\perp,4}$ = 1.4 ± 0.5	8° ± 2°	3.5 ± 1[g]

[a] The internuclear axis z'' of the stressed $H_A(Li^+)$ center makes an angle $\theta'' = 24° \pm 1°$ with [100] in the (011) plane.
[b] The symmetry axis of the g tensor is taken to coincide with the Cl_2^- internuclear axis z''.
[c] For $\vec{A}_1$: $\theta_1'' \cong 32°$ with [100] and approximately in (001) plane.
[d] For $\vec{A}_3$: $\theta_3'' \cong 73°$ with [100] and approximately in (001) plane.
[e] For $\vec{A}_2$: $\theta_2'' \cong 16°$ with [100] and approximately in (001) plane.
[f] For the orientations of the various symmetry and tensor axes of the unstressed $H_A(Li^+)$ center see Figs. 3 and 4(a) and Refs. 1 and 2.
[g] This is the reduced linewidth (see Refs. 1 and 2).

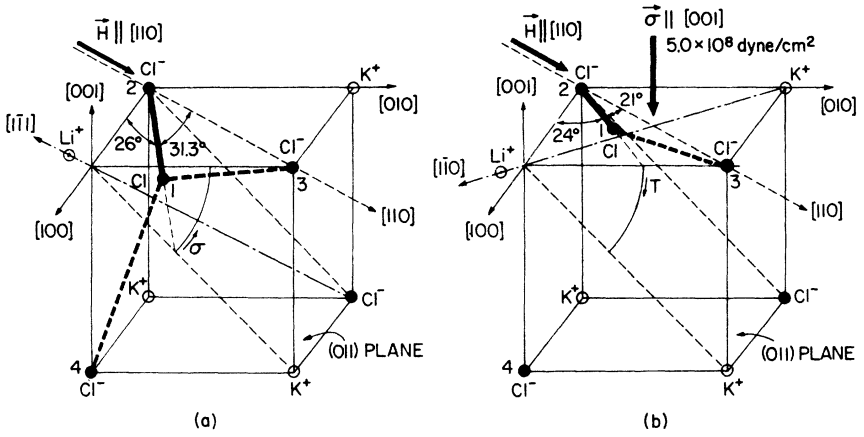

FIG. 4. (a) Schematic representation of the unstressed $H_A(Li^+)$. This model is identical to the one shown in Fig. 3 except that it is drawn in another orientation; σ indicates the path that the Cl_2^- describes when [001] uniaxial stress is applied; (b) schematic model of the $H_A(Li^+)$ center under high [001] stress ($\sim 5\times10^8$ dyn/cm^2) at 4.2 K; T indicates the return path of the Cl_2^- as the temperature is raised.

Figure 2(b) shows that the effect of the [001] stress on the $\vec{H} \parallel [100]$ spectrum is also quite noticeable but less drastic. The positions of most of the $\theta = 26°$ lines have remained virtually unchanged and the stress has merely produced a not-so-well-resolved shf structure. A careful inspection of this shf structure leads to the conclusion that there is a very small ($\lesssim 2$ G) shf interaction with a *fourth* Cl nucleus. The effect is too small, however, for further quantitative analysis.

The integrated intensity at low microwave powers of the $\theta = 24°$ spectrum of the stressed $H_A(Li^+)$ center [Fig. 2(b)] is, within the experimental error of $\pm 5\%$, equal to the integrated intensity of the $\theta = 26°$ spectrum of the unstressed $H_A(Li^+)$ [Fig. 1(a)]. This indicates that the change of the $H_A(Li^+)$-center geometry by the $\vec{\sigma} \parallel [001]$ stress completely overwhelms any effect that the $\vec{\sigma} \parallel [001]$ stress could have had on the three tunneling orientations of the C_{3v} RIM.

Finally, the stressed $H_A(^6Li^+)$ center was investigated in a KCl crystal doped with Li containing 99.3% ^{6}Li (Li normally contains 92.6% ^{7}Li). No difference was observed between the stressed $H_A(^6Li^+)$ center and the stressed $H_A(^7Li^+)$ center.

B. Model of the stressed $H_A(Li^+)$ center

It is clear from the results of the Sec. III A that the geometry of the $H_A(Li^+)$ center has been drastically changed by the ⟨100⟩ uniaxial stress. On the other hand it is reasonable to assume that the basic constituents of the center have remained unchanged: The stressed $H_A(Li^+)$ is still composed of a Cl_2^- in a negative-ion vacancy next to a substitutional Li^+ ion. The properties of the hf interaction indicate that the Cl_2^- molecular axis z'' lies in (or at least very close to) the (001) plane perpendicular to the [001] stress axis. The geometry of the stressed $H_A(Li^+)$ center then is represented schematically in Fig. 4(b). It is a Cl_2^- molecule ion which makes a 24° angle with [100] in the (001) plane and which occupies a single negative-ion site next to a substitutional Li^+ ion. Figure 4(a) represents the schematic model of the unstressed $H_A(Li^+)$ center whose molecular axis is still in the (011) plane. The EPR results as such do not tell which of the two Cl nuclei of the Cl_2^- is closer to the Li^+ in the stressed $H_A(Li^+)$ center. However, through a comparison of the properties of the unstressed $H_A(Li^+)$ center with those of the $H_A(Li^+)$-type $BrCl^-$ center in KCl,[6] it was possible to establish that in the unstressed $H_A(Li^+)$ center the Cl nucleus No. 1 possessing the largest hf interaction ($A_{\parallel,1} = 106.5$ G) and making the largest angle ($\theta_1' = 30°$) with the [100] direction is closest to the Li^+ ion as shown in Fig. 4(a). It seems very reasonable to assume then that the same holds true for the stressed $H_A(Li^+)$ center. It is proposed and shown explicitly in Figs. 4(b) and 5(a) that Cl nucleus No. 1 ($A_{\parallel,1} = 108.2$ G and $\theta_1'' \cong 32°$) is closest to the Li^+ ion.

The next question is which of the surrounding Cl nuclei are responsible for the shf interaction. To answer this it is instructive to compare Figs. 5(a) and 5(b). The latter represents schematically the $H_A(Na^+)$ center (or V_1 center in an older notation[7]) in KCl: Na^+. The $H_A(Na^+)$ EPR spectrum exhibits shf structure which was shown to originate[7] from Cl nuclei Nos. 3 and 4, with nucleus No. 3 being responsible for the larger ($A_{\parallel,3} = 13.7$ G) shf interaction. Comparison of Figs. 5(a) and 5(b) clearly shows that the $H_A(Li^+)$ symmetry under stress is *qualitatively* the same as the $H_A(Na^+)$-center geometry. By analogy it is concluded then that the shf structure originates from an overlap of the Cl_2^- wave function with Cl^- ions Nos. 3 and 5 in Fig. 5(a), with the larger ($A_{\parallel,3} = 8.5$ G) shf originating from Cl^- ion No. 3 and the smaller ($A_{\parallel,5} \leq 2$ G) shf interaction [only barely visible in the $\vec{H} \parallel \langle 100 \rangle$ spectrum in Fig. 2(b)] originating from Cl^- ion No. 5. The essential features of the geometric structure of the $H_A(Li^+)$ center under sufficiently large

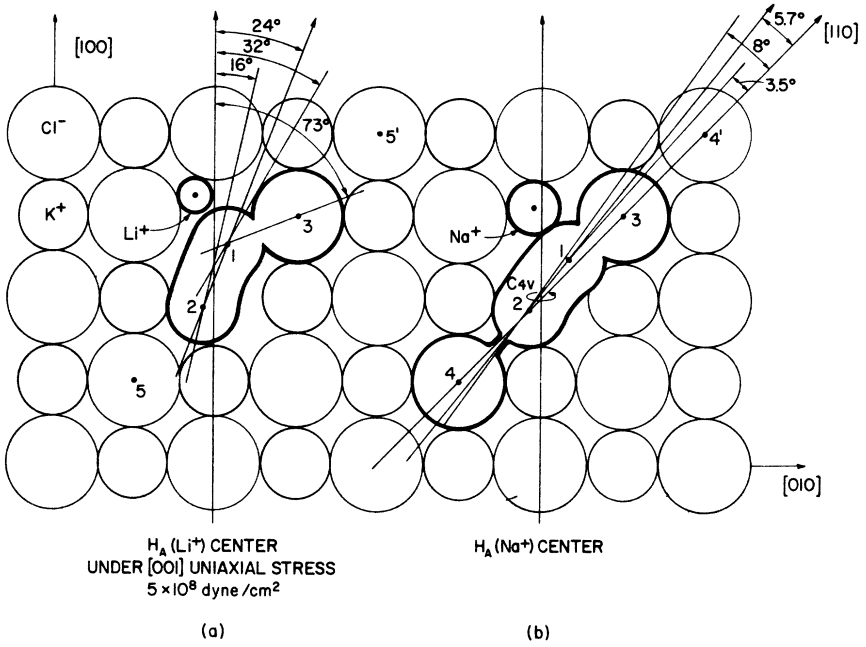

FIG. 5. (a) Schematic two-dimensional model in the (001) plane of the H_A (Li^+) center in KCl : Li^+ under high uniaxial stress along [001] at 4.2 K; (b) schematic model of the H_A (Na^+) center in KCl : Na^+.

⟨100⟩ uniaxial stress are thus determined.[8]

C. Effect of varying stress

In order to establish the geometry of the stressed $H_A(Li^+)$ center only two extreme experimental cases were considered in the foregoing sections: (a) no uniaxial stress, and (b) very high ($\sim 5\times10^8$ dyn/cm^2) uniaxial ⟨100⟩ stress. This resulted in two well-defined geometric configurations of the $H_A(Li^+)$ center. However, it is not so that these two configurations are discrete, in the sense that the uniaxial stress builds up one configuration at the expense of the other. This would be the behavior if the degeneracy of discrete tunneling orientations were lifted by uniaxial stress. If this were the case, one would for intermediate stresses (including $\sigma = 0$) observe, e.g., *both* EPR spectra represented in Figs. 1(a) and 1(b) at the same time, with relative intensity ratios determined by the magnitude of the stress.

This is not observed, however. It is, furthermore, hardly acceptable that two EPR spectra which are qualitatively and quantitatively so much different would correspond to two degenerate tunneling orientations. What is observed is that at all intermediate stresses only *one* spectrum exists whose line positions and shapes are intermediate between those represented in Figs. 1(a) and 1(b). In other words, at 4.2 K the change from one $H_A(Li^+)$ geometry to the other [(Fig. 4(a)→ Fig. 4(b)] takes place along a continuous path, and the position on this path is a function of the strength of the applied stress. The angle θ'' between the Cl_2^- internuclear axis and the [100] direction is 26° and 24°, for no stress and maximum stress, respectively. To a first approximation then, one can say that this angle θ'' has not been changed by the uniaxial stress. Consequently, the effect of the uniaxial stress on the $H_A(Li^+)$ center can be visualized as follows: With increasing [001] stress the Cl_2^- moves out of the (011) plane and the internuclear axis describes an octant of a cone around [100] whose apex angle $2\theta''$ is $\sim 2\times26° = 52°$. At very high stresses the Cl_2^- axis approaches (asymptotically no doubt) the (001) plane perpendicular to the stress direction.

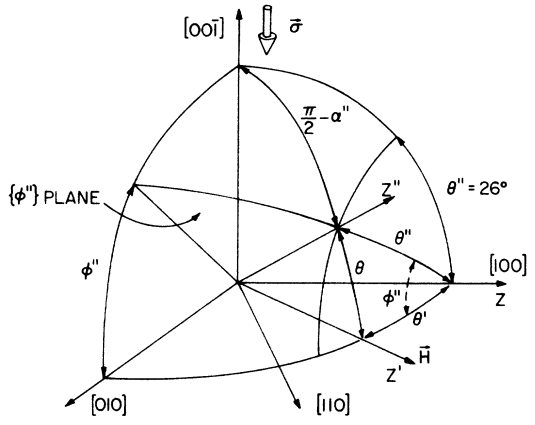

FIG. 6. Various angles used in the analysis of the effect of $\vec{\sigma} \parallel$ [001] uniaxial stress on the H_A (Li^+) internuclear axis z''. The plane defined by z'' and [100] is called the $\{\varphi''\}$ plane.

A quantitative analysis was made of this effect. The measurements are somewhat tedious, and consequently this study was limited to one temperature, viz., 4.2 K. The parameter chosen to plot against the magnitude of the stress $\vec{\sigma}$ was the angle φ'' between the (001) plane and the plane defined by the Cl_2^- axis z'' and the [100] direction (Fig. 6). This plane is called the $\{\varphi''\}$ plane. This choice of angle is neither unique nor is it necessarily the physically most relevant one, but it is an angle that is easily visualized. Another choice could have been the angle α'' between the Cl_2^- axis z'' and the (001) plane, or the angle β'' between (001) and the Li^+-Cl(1) direction (Fig. 4). However, both directions lie in the $\{\varphi''\}$ plane and α'' and β'' are proportional to φ''.

There are two ways, both very approximate, to determine φ'' for a given stress $\vec{\sigma}$. Both involve the following simplifying assumptions: (a) The Cl_2^- axis z'' in the $\{\varphi''\}$ plane describes an octant of a cone around [100]; (b) the bending and the change in bending of the Cl_2^- bond may be neglected; (c) the magnitudes of the hf and g parameters are not affected by σ. In the first method, called the (θ, θ'') method, one keeps the magnetic field $\vec{H}$ parallel to [110] and one records the EPR spectra for various stresses. From the magnitude of the hf interaction (determined by the difference between the lowest and the highest line of the EPR spectrum) one calculates θ, the angle between $\vec{H}$ and the Cl_2^- axis z'', using the well-known formula $K^2g^2 = A_{\parallel}^2 g_{\parallel}^2 \cos^2\theta + A_{\perp}^2 g_{\perp}^2 \sin^2\theta$. The angle φ'', using Fig. 6, is then given by

$$\cos\varphi'' = \frac{\cos\theta - \cos 45^\circ \cos\theta''}{\sin 45^\circ \sin\theta''} ,$$

in which θ'' is the angle (26° to 24°) between the Cl_2^- internuclear axis z'' and the [100] direction. In the second method, called the (θ', θ'') method, one determines which angle θ' between $\vec{H}$ and $\hat{z} \parallel [100]$ in the (001) plane produces a maximum in the Cl_2^- hf interaction. In this case φ'' is given by

$$\sin^2\varphi'' = \frac{\cos^2\theta' - \cos^2\theta''}{\cos^2\theta' \sin^2\theta''} .$$

This latter method is, in principle, not more accurate than the former one and because it is more tedious (each determination of θ' requires an angular-variation study) it was not applied. It could be used as a check for the results of the (θ, θ'') method. Both methods become rather insensitive in the determination of φ'' when the $\{\varphi''\}$ plane containing the Cl_2^- axis approaches the (001) plane to within ~5°. For these small φ'' angles one should really perform an angular-variation study in the $(\vec{H}, z'')$ plane perpendicular to the (001) plane. However this was not possible with our experimental setup, in which $\vec{H}$ was always in the (001) plane.

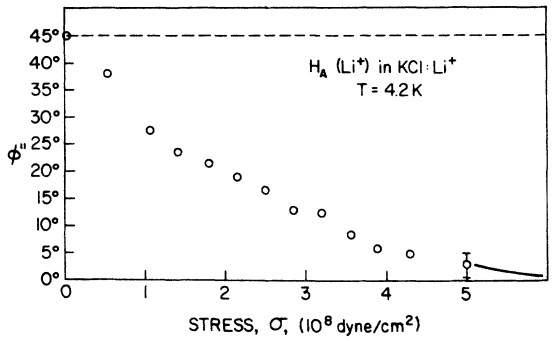

FIG. 7. Relationship at 4.2 K between the strength of the $\vec{\sigma} \parallel$ [001] uniaxial stress and the angle φ'' defined in Fig. 6.

Because of the strongly varying width and shape of the EPR lines, the measurements cannot be done very accurately. Furthermore, the three simplifying assumptions are only approximately fulfilled. Consequently, there is a rather large spread in the precision of the calculated φ'' values. Figure 7 presents the results obtained with the (θ, θ'') method. This graph suggests (a) that φ'' will tend to zero for high stresses, and (b) that for the highest stresses used in this experiment, φ'' (at 4.2 K) is not larger than ~5°, and possibly smaller. Thus, for most practical purposes, the Cl_2^- may be considered to lie in the (001) plane at 4.2 K for these high stresses.

D. Effect of varying temperature

The effect of increasing temperature on the EPR spectra of the unstressed $H_A(Li^+)$ center is very interesting and its analysis has been presented in great detail in II. We have also investigated the effect of temperature on the EPR spectrum of the ⟨100⟩ stressed crystal. The following experiment was performed: A crystal was stressed along [001] with a large stress ($\sigma = 5\times10^8$ dyn/cm²) and the EPR spectrum was followed as a function of temperature. Using the (θ, θ'') method, φ'' was determined as a function of temperature. Figure 8 presents the results. It is observed that increasing the temperature counteracts the effect of the [001] uniaxial stress, while decreasing the temperature aids it. In other words, increasing the temperature of the stressed crystal pushes the Cl_2^- axis z'' away from the (001) plane and back toward the (011) plane. All indications are that this return takes place along the same path, i.e., along the octant of a cone with a $2\theta'' \approx 52°$ apex angle. Whether the Cl_2^- axis returns completely into the (011) plane is very much dependent upon the magnitude of $\vec{\sigma}$. If the uniaxial stress applied at 4.2 K is high (~5×10^8 dyn/cm²) one finds

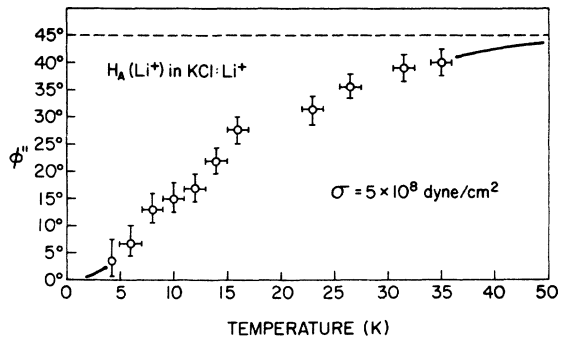

FIG. 8. Effect of temperature on the orientation of the [001] stressed $H_A(Li^+)$ center. The angle φ'' is defined in Fig. 6.

(Fig. 8) that with increasing temperature the Cl_2^- axis approaches, asymptotically very likely, the (011) plane. Figure 1(c) presents the $\vec{H} \parallel [110]$ EPR spectrum at $T = 27$ K for $\sigma = 5\times10^8$ dyn/cm^2. Comparison with Fig. 1(a) shows distinct qualitative and quantitative differences which are a consequence of the fact that φ'' has not yet reached the 45° value at this temperature. Also at 35 K the Cl_2^- axis has very clearly not yet returned into the (011) plane. However, around and above 35 K the specimens are crushed by the uniaxial stress.

The data suggest that for all practical purposes, the Cl_2^- axis of the stressed $H_A(Li^+)$ center lies in the (011) plane above ~ 50 K. As a check, the following experiment was done at 77 K: The motionally averaged EPR spectrum of $H_A(Li^+)$ [Fig. 5(a) in II] was monitored as the uniaxial stress was varied from 0 to about 3×10^8 dyn/cm^2, at which point the sample usually crushed. At this high temperature the uniaxial stress did not seem to exert any effect whatsoever on the averaged $H_A(Li^+)$ EPR spectrum. Consequently $\vec{\sigma}$ is not effective in changing the center geometry if the temperature is sufficiently high. Furthermore, with stress coupling coefficients of normal magnitude[4] (~ 2×10^{-24} cm^3), 77 K is too high a temperature to see an effect of $\vec{\sigma}$ on the lifting of the degeneracy of the RIM orientations.

With reference to Figs. 7 and 8 one can summarize this section by saying that the φ'' vs $\vec{\sigma}$ curve will become less steep as the temperature is raised and that it becomes a horizontal line when the temperature becomes sufficiently high (at least 50 or 60 K). On the other hand, for $T < 4.2$ K the curve is steeper and $\varphi'' \approx 0°$ is reached for lower stresses, as was verified experimentally.

E. Restricted interstitial motion (RIM) of the stressed $H_A(Li^+)$ center

In Sec. IIIB it was pointed out that the heavily [001] stressed $H_A(Li^+)$ center in KCl : Li$^+$ has qualitatively the same symmetry as the $H_A(Na^+)$ center in KCl : Na$^+$. The latter has been shown[2,7] to possess two distinct reorientation motions: (a) a restricted interstitial motion (RIM) of C_{2v} symmetry around ⟨110⟩, and (b) a pyramidal motion (PM) of C_{4v} symmetry around ⟨100⟩.

It is clear that the stressed $H_A(Li^+)$ center cannot exhibit a PM of C_{4v} symmetry around [100] because the [001] stress is perpendicular to this [100] direction and therefore does not permit it. However, a comparison of Figs. 5(a) and 5(b) indicates that the stressed $H_A(Li^+)$ could very well have a RIM of C_{2v} symmetry around ⟨110⟩. This latter motion, in the case of $H_A(Na^+)$, was shown to be the following: The interstitial Cl atom No. 1 in Fig. 5(b) is being exchanged between substitutional Cl$^-$ ions Nos. 2 and 3 [see Fig. 10 in II]; i.e., the interstitial exchanges molecular bonds with these two ions. This RIM motion of $H_A(Na^+)$ is thermally activated at higher temperatures and gives rise to lifetime broadening of the EPR lines at and above 36 K.

The evidence supporting the conclusion that the stressed $H_A(Li^+)$ center possesses a C_{2v} RIM around ⟨110⟩ came from the observation that the EPR lines of the stressed center show lifetime broadening at and above $T_{LB} = 30 \pm 2$ K. The determination of T_{LB} was done on one of the outer $\vec{H} \parallel [100]$ EPR lines (Fig. 2) which, in this temperature range, have virtually the same shape and width as those of the unstressed $H_A(Li^+)$ lines. In other words, at 29 K Fig. 2(b) looks virtually identical to Fig. 2(a). This temperature is, within experimental error, equal to the T_{LB} (RIM) $= 29 \pm 1$ K temperature at which the rapid RIM of the unstressed $H_A(Li^+)$ gives rise to lifetime broadening of the EPR lines. In the latter case a motionally averaged $H_A(Li^+)$ EPR spectrum resulted at 77 K, from which the geometry of the RIM could be unambiguously derived. For the stressed $H_A(Li^+)$ center one could have expected that motional averaging would result in a Cl_3^{-2} EPR pattern with ⟨110⟩ as a symmetry axis because the absence of a C_{4v} pyramidal motion here would not spoil the observation of this averaging process as did happen for $H_A(Na^+)$ in KCl : Na$^+$. However, averaging into a Cl_3^{-2} pattern [involving Cl ions Nos. 1–3 in Fig. 5(a)] is not observed. We saw in Sec. IIID that at 30 K, where the lifetime broadening starts, the stressed $H_A(Li^+)$ center is well on its way back to the geometry of the unstressed $H_A(Li^+)$ center (Fig. 8). In fact, at 77 K the RIM of the stressed $H_A(Li^+)$ has become identical to the RIM of the unstressed center because, as we saw, at this temperature no effect of the uniaxial stress on the averaged EPR spectrum can be observed. Consequently, for a given [001] stress there must be a temperature for the stressed $H_A(Li^+)$ center for

which Cl^- ion No. 4 starts to get involved in the RIM. Clearly, the Cl_2^- must have returned quite close to the (011) plane in order for this to happen, but a precise determination of this position and the corresponding temperature cannot be determined by the EPR measurements alone.

Since the C_{3v} RIM of the unstressed $H_A(Li^+)$ center is tunneling at very low temperatures, one may ask whether the C_{2v} RIM of the stressed $H_A(Li^+)$ is not also tunneling at low temperatures. EPR measurements alone cannot prove or disprove this, but there is at least one observation which indicates that the RIM of the stressed $H_A(Li^+)$ may be tunneling at low temperatures. The lifetime broadening temperatures of both the stressed and unstressed $H_A(Li^+)$ centers are the same (~ 29 K) within experimental error. Admittedly, at 29 K one is in the Arrhenius regime for both RIM's, but it does not seem unreasonable to extrapolate the similarity to lower temperatures and thus propose that the RIM of the stressed $H_A(Li^+)$ is tunneling too at liquid-helium temperatures.

In this connection another observation should be mentioned which may or may not be connected with the tunneling character of the RIM of the stressed $H_A(Li^+)$. In II, attention was drawn to the fact that the spin-lattice relaxation time T_1 of $H_A(Li^+)$ is surprisingly short. A very rough estimate gave $T_1 \approx 5\times10^{-5}$ sec. Our measurements indicate that T_1 remains at least as short in the stressed $H_A(Li^+)$ center. (Actually, our observations suggest that stresses up to $\sim 3\times10^8$ dyn/cm^2 shorten T_1 even more.) The tunneling and the short T_1 may or may not be connected. It is remarkable to mention though that the $H_A(Li^+)$-type $BrCl^-$ center in a KCl: (Li^+, Br^-) crystal has virtually the same geometric structure as the unstressed $H_A(Li^+)$ center[6]; however, it has an easily saturable EPR spectrum at 4.2 K, indicating a rather long T_1, and it does *not* possess a RIM, let alone a tunneling one.

IV. UNIAXIAL-STRESS OBSERVATIONS ON OTHER $H_A(Li^+)$ CENTERS

A. $H_A(Li^+)$-type $BrCl^-$ center in KCl

The $H_A(Li^+)$-type $BrCl^-$ center in KCl: (Li^+, Br^-) has a structure which is in most details the same as the unstressed $H_A(Li^+)$ center,[6] except that one is dealing with a $BrCl^-$ molecule ion instead of a Cl_2^-. The tipping angle with respect to the [100] direction in the (011) plane and the bending of the molecular bond are almost identical for both centers. It was shown that the Br side of the $BrCl^-$ occupies the more substitutional position No. 2 in Fig. 3 while the Cl occupies the more interstitial position No. 1.

A $\vec{\sigma} \parallel [001]$ uniaxial-stress experiment was performed at 4.2 K on the $H_A(Li^+)$-type $BrCl^-$ center to see if its geometric structure would change too. The result of the experiment was the following: The [001] uniaxial stress did not seem to affect the $H_A(Li^+)$-type $BrCl^-$ in any way. The reasons for the different behavior of these two centers under stress are not known, and we can only list here some subtle but possibly significant differences between these otherwise so similar centers. The $H_A(Li^+)$-type $BrCl^-$ center (a) does not possess a RIM motion (this can be attributed to the fact[6] that the Br does not occupy the more interstitial position No. 1 in Fig. 3), and (b) does not possess preferential weak molecular bonds with substitutional Cl^- ions Nos. 3 and 4.

B. $H_A(Li^+)$ center in NaF: Li^+

The structure of the $H_A(Li^+)$ center in NaF: Li^+ was recently determined by Plant and Mieher.[9] Its structure is somewhat different from the $H_A(Li^+)$ center in KCl: Li^+. The center consists of a F_2^- molecule ion on a single anion site next to a substitutional Li^+. However, the F_2^- internuclear axis makes a 14.1° angle with the [110] direction and lies in a plane through this [110] direction which makes a 33.2° angle with the (001) plane. In other words, the F_2^- axis makes a $\theta'' = 33.9°$ angle with [100] and lies in a $\{\varphi''\}$ plane through this direction which makes a $\varphi'' = 13.8°$ angle with the (001) plane. There is furthermore a shf interaction with a third F nucleus. One can take the viewpoint then that the $H_A(Li^+)$-center structure in NaF: Li^+ corresponds to an orientation of the stressed $H_A(Li^+)$ center in KCl: Li^+ at some intermediate stress, with the difference that the cone has a $2\theta'' = 2\times33.9° = 67.8°$ apex angle, instead of ~ 52°.

With this in mind $\vec{\sigma} \parallel [001]$ uniaxial-stress experiments were performed on this $H_A(Li^+)$ center in NaF: Li^+ at and above 4.2 K. The expectation was that possibly the F_2^- molecular axis could be pushed completely into the (001) plane. However, the experiments showed clearly that the stress did not affect the geometric structure of the center at all.

V. SUMMARY AND CONCLUSION

The important results of the foregoing sections can be summarized as follows:

(i) [001] uniaxial stress drastically changes the geometric structure of the $H_A(Li^+)$ center in KCl: Li^+. At liquid-helium temperatures the stress pushes the Cl_2^- internuclear axis out of the (011) plane into the (001) plane [Figs. 4(b) and 5(a)].

(ii) The Cl_2^- axis z'' describes a continuous path as a function of stress. This path is an octant of a cone with [100] as its axis and with a ~ 52° apex angle [Fig. 4(a)].

(iii) Raising the temperature counteracts the

effect of uniaxial stress: The Cl_2^- axis is pushed back toward the (011) plane in a continuous way along the same octant of the cone [Fig. 4(b)]. At 77 K, the uniaxial stress does not affect the $H_A(Li^+)$ center in any discernible way.

(iv) The stressed $H_A(Li^+)$ center possesses a restricted interstitial motion (RIM) of C_{2v} symmetry around ⟨110⟩ and it seems quite probable that this is a tunneling motion at liquid-helium temperatures.

(v) The geometric structures of the $H_A(Li^+)$-type $BrCl^-$ center in KCl and the $H_A(Li^+)$ center in NaF : Li^+ which have geometric structures quite similar to the $H_A(Li^+)$ center in KCl : Li^+ are not at all influenced by ⟨100⟩ uniaxial stress.

The central remaining question now is what are the reasons why ⟨100⟩ uniaxial stress changes the geometric structure of the $H_A(Li^+)$ center in KCl. In view of the fact [see (iv) above] that centers with almost identical or very similar symmetry are not affected in this manner by uniaxial stress, one can rule out an explanation based solely on the gross symmetry features of the center. We tend to the conclusion that there is a subtle balance of forces within and around the $H_A(Li^+)$ center in KCl : Li^+ which is rather unique to the center itself. The ⟨100⟩ uniaxial stress disrupts this subtle balance and results in a deformation of the center.

ACKNOWLEDGMENTS

The author wants to thank E. L. Yasaitis for constructing the uniaxial-stress apparatus, P. H. Yuster and C. J. Delbecq for many discussions, and E. Hutchinson for growing the crystals used in these experiments.

---

*Based on work performed under the auspices of the U. S. Atomic Energy Commission.

†Present address.

[1]D. Schoemaker and J. L. Kolopus, Phys. Rev. B 2, 1148 (1970).

[2]D. Schoemaker and E. L. Yasaitis, Phys. Rev. B 5, 4970 (1972).

[3]For recent surveys of hole and interstitial centers in alkali halides see M. N. Kabler, in *Point Defects in Solids*, edited by J. H. Crawford and L. M. Slifkin (Plenum, New York, 1972); N. Itoh, Cryst. Lattice Defects 3, 115 (1972).

[4]D. Schoemaker, Bull. Am. Phys. Soc. 18, 305 (1973).

[5]See also Ref. 26 in Ref. 2.

[6]D. Schoemaker and C. T. Shirkey, Phys. Rev. B 6, 1562 (1972).

[7]C. J. Delbecq, E. Hutchinson, D. Schoemaker, E. L. Yasaitis, and P. H. Yuster, Phys. Rev. 187, 1103 (1969).

[8]Actually, the statement that the geometry of the $H_A(Li^+)$ center under high $\vec{\sigma} \parallel [001]$ uniaxial stress is determined holds only for $\frac{2}{3}$ of the $H_A(Li^+)$ centers, namely, for those whose orientations are, or are equivalent with, the 1-2 and 1-3 orientations in Fig. 4(a). The behavior under $\vec{\sigma} \parallel [001]$ stress of the $H_A(Li^+)$ in the 1-4 orientation could not be investigated. The reason is that our experimental setup was limited to the $\vec{H} \perp \vec{\sigma}$ configuration. In this configuration the angle between $\vec{H}$ and the 1-4 Cl_2^- axis varies between $\theta = 90°$ and $\theta = 64°$ when the magnetic field is rotated in the (001) plane. Such large angles result in very contracted EPR spectra, the details of which are overshadowed by the more extended $\theta = 26°$ (when $\vec{H} \parallel [100]$) and $\theta = 31.3°$ (when $\vec{H} \parallel [110]$) spectra (see Figs. 1 and 2). It seems likely though that the $\vec{\sigma} \parallel [001]$ stress does not affect the structure of the $H_A(Li^+)$ center in the 1-4 orientation.

[9]W. Plant and R. L. Mieher, Phys. Rev. B 7, 4793 (1973).